

BNL--38621

BNL-38621

DE87 001376

STRANGE PARTICLE PRODUCTION IN NEUTRINO-NEON  
CHARGED CURRENT INTERACTIONS

Received by  
OCT 27 1986

Presented by R. Plano, Rutgers University at The 12th International  
Conference on Neutrino Physics and Astrophysics, Sendai, Japan, June 86

N. J. Baker, P. L. Connolly, S. A. Kahn, M. J. Murtagh, R. B. Palmer,  
N. P. Samios, and M. Tanaka, Brookhaven National Laboratory

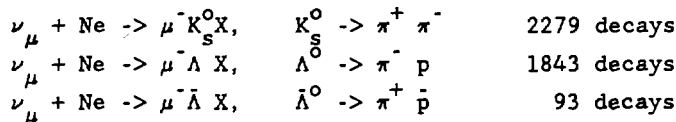
C. Baltay, M. Bregman, L. Chen, M. Hibbs, R. Hylton, J. Okamitsu, and  
A. C. Schaffer, Columbia University

M. Kalelkar, Rutgers University

(Expanded version to be published in Physical Review D, 1 Sep, 1986)

I. INTRODUCTION.

Neutral strange particle production in charged-current  $\nu_\mu$   
interactions have been studied in the Fermilab 15-foot neon bubble  
chamber. The reactions studied included:



Associated production is expected to be the major source of  
strange particles in charged-current neutrino interactions since the  
d-quark is the only valence quark the neutrino interacts with, and  
makes a strange quark only via a Cabibbo disfavored process; strange  
quarks must be ejected from the sea. Other processes, such as charm  
production and interactions with sea quarks are expected to be small.

The sample described here, from 61,800 charged-current events, is  
used to provide insight into these ideas. Other topics include:

the first clear observation of  $\Sigma^0$  production (94 examples) and  $\Xi^-$  production (4 examples) by neutrinos.

the dependence on various leptonic and hadronic variables is investigated.

a fit to single and associated production of  $s$ ,  $s/\bar{s}$ , and  $c$  quarks is described based on the numbers of single and double strange particle production events.

## II. EXPERIMENTAL PROCEDURE

The beam used in this experiment was the Fermilab double horn-focussed wide band  $\nu_\mu$  beam. The primary proton beam was extracted at an energy of 400 GeV in a fast spill ( $\sim 20 \mu\text{sec}$ ) with an average intensity of  $10^{13}$  protons per pulse incident on the production target. The resulting neutrino spectrum peaked at 23 GeV, with about 10% of the events above 100 GeV; the average neutrino energy was 46 GeV.

The detector was the Fermilab 15-foot bubble chamber filled with a "heavy" neon-hydrogen mixture (61% atomic neon). The chamber liquid had a radiation length of 40 cm, so that electrons were easily identified providing a clear distinction between  $\gamma$  pair production and neutral strange particle decay ( $V^0$ ). All  $\gamma$ 's were measured to estimate the  $\pi^0$  energy in each event. The interaction length was 125 cm providing a clean identification of muons; the fastest negative leaving track in each event was taken to be the muon. The "punch-through" of pions which thereby simulated muons was 9.1%.

The film was scanned for all charged current events having at least one  $V^0$ . To be accepted, an event had to meet the following criteria:  $\mu^-$  momentum greater than 2 GeV/c,  $V^0$  length greater than 1 cm,  $V^0$  potential length greater than 10 cm, and visible energy in excess of 10 GeV.

All such events were measured and processed through our version of the geometrical reconstruction program TVGP and the kinematic fitting program SQUAW. For each  $V^0$  the following hypotheses were

tried as constrained fits to the production vertex:  $K_S \rightarrow \pi^+ \pi^-$ ,  $\Lambda \rightarrow p \pi^-$ ,  $\bar{\Lambda} \rightarrow \pi^+ \bar{p}$ , and  $\gamma p \rightarrow (p) e^+ e^-$ . Fits were required to have two or three degrees of freedom, and a  $\chi^2$  less than five times the number of constraints.

This sample of events, consisting of 2279  $K_S$ , 1843  $\Lambda$ , and 93  $\bar{\Lambda}$ , will be referred to as the strange charged-current (SCC) sample. It will be compared with a random charged-current (RCC) sample, selected randomly, without regard to the presence or absence of strangeness. After all cuts, the RCC sample consisted of about 2500 events.

The measurement of events in both samples included all the charged tracks at the primary vertex, and all the visible associated neutrals ( $\gamma$ 's,  $V^0$ 's and neutron interactions). We then corrected for the estimated 20% of the hadronic energy missing<sup>1</sup>.

### III. PRODUCTION RATES

To calculate  $V^0$  production rates, it was necessary to correct the observed number of  $V^0$ 's for various efficiencies and backgrounds. The ten correction factors included corrections for geometric detection efficiency, interaction before decay, low-lifetime loss, slow decay prong, punch-through background, fake fits, random scan efficiency, reconstruction efficiency, branching ratio, and ambiguity resolution. The major contribution comes from the branching ratio to undetected (all neutral) decay modes which is well known; it includes a factor of 2 for  $K_L$ , so that our "K<sup>0</sup>" rates include  $K^0$  and  $\bar{K}^0$ . The average total weights are  $K^0$ :  $4.56 \pm 0.23$ ,  $\Lambda$ :  $2.18 \pm 0.12$ , and  $\bar{\Lambda}$ :  $3.08 \pm 0.41$ .

Inclusive  $V^0$  production rates as a fraction of all charged-current events are shown in Table I. They are based on a total charged-current sample of  $61800 \pm 2800$  events with  $E_\nu > 10$  GeV and  $P_\mu > 2$  GeV/c.

In Table II we give the observed number of events and corrected rates for 11 specific single-, double-, and triple- $V^0$  production channels. The rates are the solutions of 11 simultaneous equations;

for example, the number of observed single- $K^0$  events is written as the sum over the true rates for each of the 11 channels multiplied by the probability for that channel to be observed as a single  $K^0$  and no other neutral strange particle.

TABLE I

Total Inclusive Strange Particle Production Rates. The  $\Lambda$  rate includes  $\Lambda$ 's from  $\Sigma^0$  decay. The  $K^0$  rate includes ( $K^0 + \bar{K}^0$ ).

Particle	Observed	Corrected	Rate per charged-current event
$K^0$	2279	10392	$0.168 \pm 0.012$
$\Lambda$	1843	4018	$0.065 \pm 0.005$
$\bar{\Lambda}$	93	286	$0.0046 \pm 0.0008$
$\Sigma^0$	94	713	$0.011 \pm 0.003$
$\Xi^-$	4	36	$(6 \pm 4) \times 10^{-4}$

TABLE II

Single, Double and Triple  $V^0$  Production Rates. Note that X does not contain a visible  $V^0$ .  $K^0$  includes  $K^0 + \bar{K}^0$ .

Reaction	Observed events	Rate per charged-current event
	Single- $V^0$	
$\nu_{\mu} \text{Ne} \rightarrow \mu^- K^0 X$	1834	$(8.0 \pm 0.8) \times 10^{-2}$
$\mu^- \Lambda X$	1569	$(3.2 \pm 0.3) \times 10^{-2}$
$\mu^- \bar{\Lambda} X$	79	$(2.4 \pm 0.6) \times 10^{-3}$
	Double- $V^0$	
$\mu^- K^0 K^0 X$	100	$(1.6 \pm 0.8) \times 10^{-2}$
$\mu^- K^0 \Lambda X$	205	$(2.3 \pm 0.4) \times 10^{-2}$
$\mu^- K^0 \bar{\Lambda} X$	6	$(1.4 \pm 0.5) \times 10^{-3}$
$\mu^- \Lambda \Lambda X$	20	$(1.6 \pm 6.9) \times 10^{-4}$
$\mu^- \Lambda \bar{\Lambda} X$	8	$(9 \pm 3) \times 10^{-4}$
	Triple- $V^0$	
$\mu^- K^0 K^0 K^0 X$	4	$(6 \pm 3) \times 10^{-3}$
$\mu^- K^0 K^0 \Lambda X$	8	$(6 \pm 2) \times 10^{-3}$
$\mu^- K^0 \Lambda \Lambda X$	5	$(2 \pm 1) \times 10^{-3}$

Strange particle production has been studied previously both in neutrino<sup>3-10,13</sup> and antineutrino<sup>8-12</sup> experiments. In Table III we compare our results with some of these earlier measurements. The statistical richness of this experiment should be emphasized; we have more events than all the other experiments combined.

TABLE III  
Comparison of Results on  $K^0$  and  $\Lambda$  production by  $\nu$  and  $\bar{\nu}$

Reference	$\langle E_\nu \rangle$ (GeV)	$N_K$	$R_K$	$N_\Lambda$	$R_\Lambda$	$R_\Lambda/R_K$
This exp. $\nu$ Ne	46	2279	$0.168 \pm 0.012$	1843	$0.065 \pm 0.005$	$0.39 \pm 0.04$
All others combined:		1980		1257		
9	$\nu$ Ne 103	203	$0.230 \pm 0.017$	98	$0.057 \pm 0.007$	$0.25 \pm 0.03$
10	$\nu$ n 62	234	$0.208 \pm 0.016$	157	$0.071 \pm 0.007$	$0.34 \pm 0.05$
10	$\nu$ p 62	154	$0.177 \pm 0.016$	77	$0.043 \pm 0.006$	$0.24 \pm 0.04$
8	$\nu$ p ~45	23	$0.15 \pm 0.04$	4		
7	$\nu$ p 43	359	$0.175 \pm 0.009$	180	$0.045 \pm 0.004$	$0.26 \pm 0.03$
5	$\nu$ p ~45	89		58		
4	$\nu$ p ~45	19		20		
6	$\nu$ d ~ 3	13	$0.024 \pm 0.009$	26	$0.028 \pm 0.010$	$1.17 \pm 0.61$
3	$\nu$ Fr ~ 3	14		40		
13	$\nu$ Fr 8	82	$0.071 \pm 0.008$	76	$0.031 \pm 0.004$	$0.43 \pm 0.07$
12	$\bar{\nu}$ Ne 81	64	$0.219 \pm 0.028$	37	$0.065 \pm 0.012$	$0.30 \pm 0.05$
13	$\bar{\nu}$ n 45	95	$0.219 \pm 0.025$	68	$0.082 \pm 0.012$	$0.37 \pm 0.07$
13	$\bar{\nu}$ p 45	193	$0.222 \pm 0.018$	113	$0.070 \pm 0.008$	$0.32 \pm 0.05$
15	$\bar{\nu}$ Ne ~45	350	$0.164 \pm 0.009$	257	$0.063 \pm 0.004$	$0.38 \pm 0.03$
11	$\bar{\nu}$ p ~45	88	$0.151 \pm 0.032$	46	$0.045 \pm 0.009$	$0.30 \pm 0.09$

$R_K$  and  $R_\Lambda$  are inclusive rates as a fraction of all charged-current events.  $N_K$  and  $N_\Lambda$  are the raw, observed numbers of  $V^0$ 's.

IV.  $\Sigma^0$  and  $\Xi^-$  Production.

The  $\Lambda\gamma$  effective mass distribution, shown in Figure 1, exhibits a very clear signal at the  $\Sigma^0$  mass. A fit to the distribution, using a Gaussian shape for the  $\Sigma^0$  and a third-order polynomial background, which had a  $\chi^2$  of 23.5 for 24 degrees of freedom, is shown as the solid line, while the dashed line indicates the fitted background. The fit yielded a total of  $94 \pm 25$   $\Sigma^0$ 's with a mass of  $M = 1195 \pm 2$  MeV and a width of  $\sigma = 8 \pm 2$  MeV. The mass is consistent with the world average<sup>2</sup> of 1192.5 MeV, and the width coincides with our mass resolution in the  $\Lambda\gamma$  system at the  $\Sigma^0$  mass.

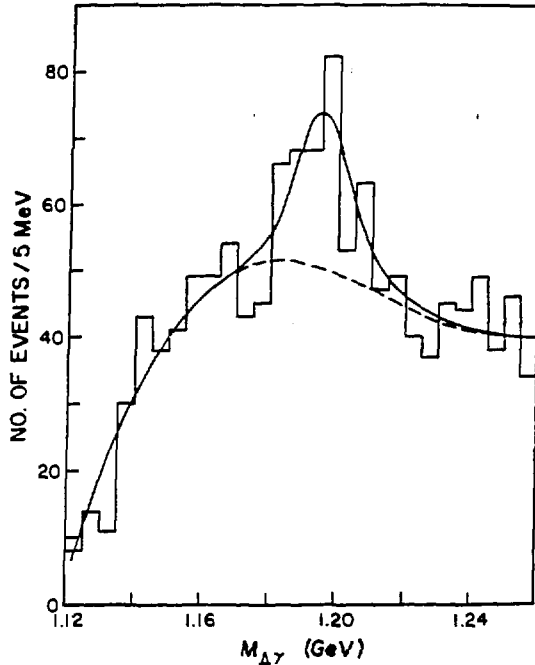


Figure 1: Effective mass of the  $\Lambda\gamma$  system, using fitted  $\Lambda$  and  $\gamma$ .

To obtain the  $\Sigma^0$  rate, it is necessary to weight the  $\Sigma^0$  for both the  $\Lambda$  and  $\gamma$  detection efficiencies. The sources of  $\gamma$  losses include (average weights given in parentheses): geometric detection efficiency (1.33), low-energy  $e^\pm$  prongs (1.16), Short projected  $e^\pm$  tracks on film (1.37), poor  $e^\pm$  track visibility (1.03), and random  $\gamma$  scan efficiency (1.69). The overall average weight for  $\gamma$ 's was  $3.18 \pm 0.31$ . The total inclusive  $\Sigma^0$  production rate is then  $(1.1 \pm 0.3)\%$  of all charged current events. The fraction of all  $\Lambda$ 's coming from  $\Sigma^0$  decay is  $(16 \pm 5)\%$ . To our knowledge, this is the first measurement of  $\Sigma^0$  production in neutrino interactions.

$\Xi^-$  production in neutrino interactions has not been previously reported. The cross section is expected to be small since double s-quark production is needed to produce a strangeness -2 particle.

Approximately one-third of the film was scanned for events in which a  $V^0$  pointed to a kink on a negative track. Candidates were measured and a kinematic fit made to the hypothesis  $\Xi^- \rightarrow \Lambda\pi^-$ ,  $\Lambda \rightarrow p\pi^-$ . In addition to the selection criteria imposed on the entire SCC sample, two additional requirements were imposed: a) the  $\Xi^-$  track length must exceed 1 cm and b) the muon candidate was required to be the fastest leaving negative track as well as the track with the largest transverse momentum with respect to the vector sum of the other track momenta. This was intended to reduce the background due to  $K_L$  interactions.

Five events satisfied all these criteria of which one was induced by  $\bar{\nu}$ . The four  $\nu$  events correspond to a rate of  $(6 \pm 4) \times 10^{-4}$  of all charged-current events including a correction of  $0.5 \pm 0.5$  events for the only significant background -- that of  $K_L$  interaction. This rate is comparable with the rate for  $\Lambda\Lambda$  production  $(1.6 \pm 6.9) \times 10^{-4}$ , which also requires two s-quarks. None of the events is compatible with  $\Xi_c$  production giving a 90%-confidence-level upper limit on the probability for producing  $\Xi_c$  times the branching ratio for the decay  $\Xi_c \rightarrow \Xi^-$  plus charged pions of  $4 \times 10^{-4}$ , expressed as a fraction of the cross section for all charged-current events.

## V. DIFFERENTIAL DISTRIBUTIONS.

To investigate strange particle production mechanisms we consider next the differential distributions for  $K^0$  and  $\Lambda$  production. To obtain the rates for these variables, we obtained distributions of each variable for the SCC and RCC samples separately, and then divided them after appropriate normalization.  $W > 2$  GeV was required in both samples to avoid the strangeness threshold.

There are striking differences between the  $K^0$  and  $\Lambda$  as illustrated by Figures 2 ( $E_\nu$ ), 3 ( $W^2$ ), and 4b ( $y_B$ ). The production

rate of  $\Lambda$  is essentially independent of  $E_\nu$ ,  $Q^2$ ,  $W^2$  and  $y_B = (E_\nu - E_\mu)/E_\nu$ , while the  $K^0$  rate increases sharply with all of these variables. A simple interpretation is that the  $\Lambda$  is produced in the target fragmentation region, and is generally independent of the energy of the  $W^+$  coming from the leptonic vertex. By contrast, the  $K^0$  is in the current jet where the  $s$  (or  $\bar{s}$ ) quark is picked up from the sea, and this process is increasingly favored as the  $W^+$  energy rises. This is in agreement with the independence of both the  $K^0$  and  $\Lambda$  rates of  $x_B$  (Figure 4).  $x_B$  is the fraction of the nucleon momentum carried by the struck quark and the production of  $K^0$  is determined primarily not by the struck quark, but rather by the  $W^+$ .

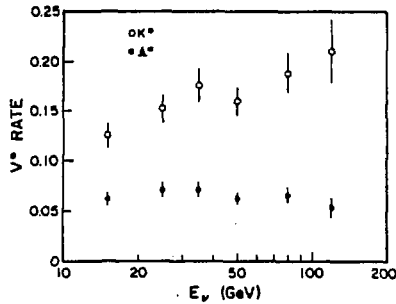


Figure 2: Inclusive  $V^0$  production rates as a function of incident neutrino energy.

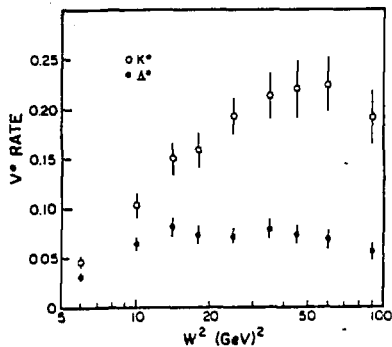


Figure 3: Inclusive  $V^0$  production rates as a function of  $W^2$ , the invariant hadronic mass squared.

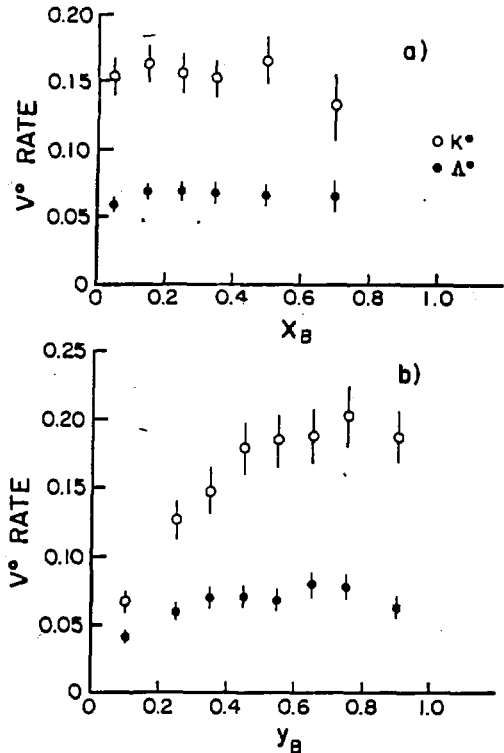


Figure 4: Inclusive  $V^0$  production rates as a function of the Bjorken scaling variables  $x_B$  and  $y_B$ .

The  $x_F$  distributions (Figure 5) show the  $\Lambda$  to be backward, characteristic of a target fragmentation process, and the  $K^0$  central but somewhat forward, as expected from its production in the current jet. The asymmetry parameters

$$A = (N_F - N_B)/(N_F + N_B)$$

are  $A_{K^0} = 0.16 \pm 0.02$  and  $A_\Lambda = -0.71 \pm 0.02$ . These are comparable to or significantly less than other experiments. The pions are produced in a narrow region around  $x_F = 0$ ; their asymmetry parameters are  $A_+ = +0.004 \pm 0.012$  and  $A_- = -0.082 \pm 0.017$ .

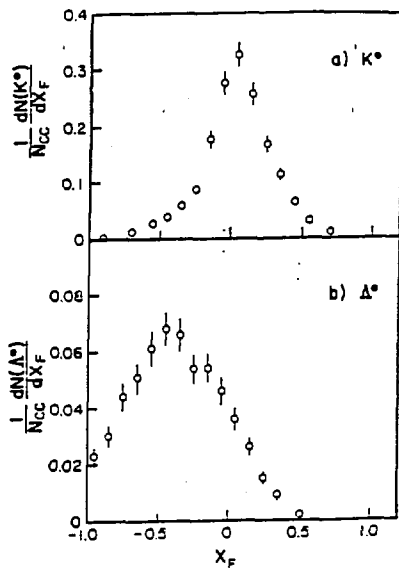


Fig. 5: Feynman  $x$  distributions for a)  $K^0$ , and b)  $\Lambda^0$ .

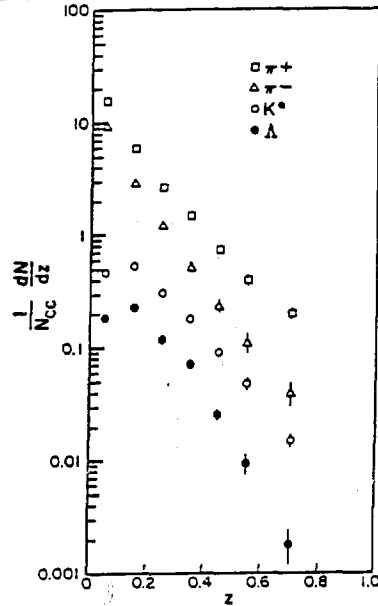


Fig. 6: Normalized distributions in the fragmentation variable  $z$  for  $K^0$ ,  $\Lambda$ ,  $\pi^+$ , and  $\pi^-$ .

Figure 6 shows the normalized  $z$  distribution for  $K^0$ ,  $\Lambda$ ,  $\pi^+$ , and  $\pi^-$ , where the fragmentation variable  $z$  is the fraction of the corrected hadronic energy carried by the particle. Note the statistically good information over more than four decades. The strange particle distributions turn over at low  $z$ , due in part to mass effects.

In the region  $0 < P_T^2 < 0.5$   $(\text{GeV}/c)^2$ , the  $P_T^2$  distributions for  $K^0$  and  $\Lambda$  can be fit by a simple exponential of the form  $A \exp(-BP_T^2)$ . QCD predicts that  $\langle P_T^2 \rangle$  should increase with  $Q^2$  and decrease with  $x_B$ . We see no such effect, as illustrated in Figure 7, whether  $P_T$  is measured relative to the  $W^+$  direction or to the experimentally more precise "lepton plane", the plane containing the neutrino and the muon,  $\langle P_T^2 \rangle_{\text{OUT}}$ . There is a clear increase with  $W^2$  at least for the  $K^0$ .

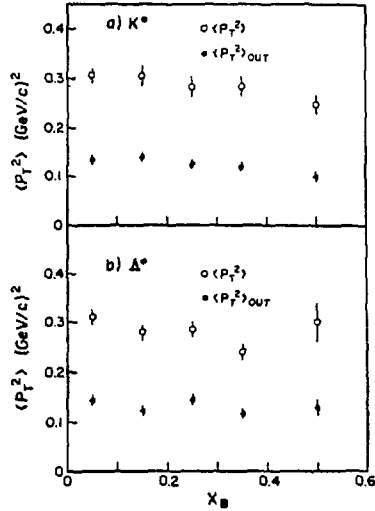


Fig. 7: Average transverse momentum squared as a function of  $x_B$ .

### VI. RATES FOR SINGLE AND ASSOCIATED S-QUARK PRODUCTION.

As described in the Introduction, the primary mechanism for strange-particle production is expected to be associated production of an  $s\bar{s}$  quark pair. It is possible to produce a single s-quark via charm production, although single  $\bar{s}$ -quark production has no simple production mechanism.

The aim of the fit described here is to use our measured rates for single- and double- $V^0$  production to derive:

$R_{AP}$ , the rate for associated production, and  
 $R_S$ , the rate for single s-quark production (via charm).

We define the following probabilities:

- $P_{SM}$  - the probability that an s-quark appears as a meson (not baryon)
- $P_{ASM}$  - the probability that an  $\bar{s}$ -quark appears as a meson (not baryon)
- $P_{MV}$  - the probability that a strange meson will appear electrically neutral (not as a  $K^+$  or  $K^-$ )
- $P_{BV}$  - the probability that a strange baryon will appear electrically neutral (not as a  $\Sigma^+$  or  $\Sigma^-$ )

We have fit the seven appropriate expressions involving these parameters to the seven single and double  $V^0$  production rates shown in Table II, excluding  $\Lambda\Lambda$ . The fit was reasonable ( $\chi^2 = 1.4$  for 2 degrees of freedom), and yielded the following results:

- $R_{AP} = 0.195 \pm 0.014$  Associated Production is dominant.  
 $R_S = 0.050 \pm 0.015$  Charm Production. Consistent with the charged-current  $\mu^-e^+$  rate of 0.5% and a roughly correct 10% branching rate for charm into  $e^+$ .  
 $P_{SM} = 0.445 \pm 0.040$   
 $P_{ASM} = 0.945 \pm 0.010$  Almost one; for an  $\bar{s}$ -quark to make an antibaryon, it must pick up two antiquarks from the sea whereas to make a meson, it needs only one u- or d-quark.  
 $P_{BV} = 0.414 \pm 0.029$   
 $P_{MV} = 0.500 \pm 0.040$  Expected, since neon is isoscalar.

Finally, we note that our fitted results, assuming associated production and charm production both take place, but double associated production does not, predict  $2.4 \times 10^{-4}$  for the  $\Lambda\Lambda$  channel (which was not used in the fit), whereas the measured rate is  $(1.6 \pm 6.9) \times 10^{-4}$ .

## VII. CONCLUSIONS.

We have studied strange-particle production in  $\nu_\mu$ -Ne charged-current interactions, using a sample of 4215 fitted  $V^0$ 's corresponding to 61,800 charged-current events. This sample is larger than all previous samples combined. Inclusive  $V^0$  production rates as a fraction of all charged-current events are measured and are shown in Tables I and II. The  $\Lambda/K$  ratio is  $0.39 \pm 0.04$  and the fraction of  $\Lambda$  coming from  $\Sigma^0$  is  $(16 \pm 5)\%$ .

The single- and double- $V^0$  production was used to determine that associated  $s\bar{s}$  production occurs at a  $(19.5 \pm 1.4)\%$  rate while single s-quark production, presumably via charm production, occurs at a  $(5.0 \pm 1.5)\%$  rate.

The  $\Lambda$  comes from target fragmentation and its rate is independent of  $E_\nu$ ,  $Q^2$ ,  $W^2$ ,  $x_B$ , and  $y_B$ . The  $K^0$  is produced in the current jet and increases with  $E_\nu$ ,  $Q^2$ ,  $W^2$ , and  $y_B$ , but is independent of  $x_B$ .

The  $P_T^2$  distribution for both the  $K^0$  and  $\Lambda$  can be described by a simple exponential. Neither  $\langle P_T^2 \rangle$  or  $\langle P_T^2 \rangle_{OUT}$  shows significant variation with  $Q^2$  or  $x_B$ , as predicted by QCD, but an increase with  $W^2$  is observed.

#### ACKNOWLEDGMENTS

We thank the scanning and measuring staffs at our institutions, and the operating crews of the 15-ft chamber and the neutrino beam at Fermilab. This research was supported by the Department of Energy (Contract No. DE-AC02-76CH00016) and by the National Science Foundation.

#### REFERENCES

1. A. Grant, Nucl. Inst. and Methods 127, 355 (1975).
2. Particle Data Group, Rev. Mod. Phys. 56, S1 (1984).
3. H. Deden et al., Phys. Lett. 58B, 361 (1975).
4. J. P. Berge et al., Phys. Rev. Lett. 36, 127 (1976).
5. J. P. Berge et al., Phys. Rev. D18, 1359 (1978).
6. N. J. Baker et al., Phys. Rev. D24, 2779 (1981).
7. H. Grassler et al., Nucl. Phys. B194, 1 (1982).
8. R. Brock et al., Phys. Rev. D25, 1753 (1982).
9. P. Bosetti et al., Nucl. Phys. B209, 29 (1982).
10. D. Allasia et al., Nucl. Phys. B224, 1 (1983).
11. O. Erriquez et al., Nucl. Phys. B140, 123 (1978).
12. V. V. Ammosov et al., Nucl. Phys. B177, 365 (1981).
13. V. V. Ammosov et al., Z. Phys. C. 30, 183 (1986).

#### DISCLAIMER

This report was prepared as an account of work sponsored by an agency of the United States Government. Neither the United States Government nor any agency thereof, nor any of their employees, makes any warranty, express or implied, or assumes any legal liability or responsibility for the accuracy, completeness, or usefulness of any information, apparatus, product, or process disclosed, or represents that its use would not infringe privately owned rights. Reference herein to any specific commercial product, process, or service by trade name, trademark, manufacturer, or otherwise does not necessarily constitute or imply its endorsement, recommendation, or favoring by the United States Government or any agency thereof. The views and opinions of authors expressed herein do not necessarily state or reflect those of the United States Government or any agency thereof.